

## Microscopic analysis of order parameters in nuclear quantum phase transitions

Z. P. Li,<sup>1,2</sup> T. Nikšić,<sup>2</sup> D. Vretenar,<sup>2,3</sup> and J. Meng<sup>1,3,4</sup>

<sup>1</sup>State Key Laboratory of Nuclear Physics and Technology, School of Physics, Peking University, Beijing 100871, People's Republic of China

<sup>2</sup>Physics Department, Faculty of Science, University of Zagreb, HR-10000 Zagreb, Croatia

<sup>3</sup>Kavli Institute for Theoretical Physics China, CAS, Beijing 100190, People's Republic of China

<sup>4</sup>School of Physics and Nuclear Energy Engineering, Beihang University, Beijing 100191, People's Republic of China

(Received 30 June 2009; published 10 December 2009)

Microscopic signatures of nuclear ground-state shape phase transitions in Nd isotopes are studied using excitation spectra and collective wave functions obtained by diagonalization of a five-dimensional Hamiltonian for quadrupole vibrational and rotational degrees of freedom, with parameters determined by constrained self-consistent relativistic mean-field calculations for triaxial shapes. As a function of the physical control parameter, the number of nucleons, energy gaps between the ground state and the excited vibrational states with zero angular momentum, isomer shifts, and monopole transition strengths exhibit sharp discontinuities at neutron number  $N = 90$ , which is characteristic of a first-order quantum phase transition.

DOI: [10.1103/PhysRevC.80.061301](https://doi.org/10.1103/PhysRevC.80.061301)

PACS number(s): 21.60.Jz, 21.10.Re, 21.60.Ev, 21.90.+f

Phase transitions in equilibrium shapes of atomic nuclei correspond to first- and second-order quantum phase transitions (QPTs) between competing ground-state phases induced by variation of a nonthermal control parameter (number of nucleons) at zero temperature. Theoretical studies have typically been based on phenomenological geometric models of nuclear shapes and potentials, or algebraic models of nuclear structure [1–3], but more recently several attempts have been made toward a fully microscopic description of shape QPT starting from nucleonic degrees of freedom [4–11]. In particular, in Refs. [7] and [8], we have reported a microscopic study of nuclear QPT in the region  $Z = 60, 62,$  and  $64$  with  $N \approx 90$ , based on constrained self-consistent relativistic mean-field (RMF) calculations of potential energy surfaces. Although in Ref. [7] the generator coordinate method was used to perform configuration mixing of angular momentum and particle-number projected relativistic wave functions restricted to axial symmetry, in Ref. [8], collective excitation spectra and transition probabilities have been calculated starting from a five-dimensional Hamiltonian for quadrupole vibrational and rotational degrees of freedom, with parameters determined by constrained mean-field calculations for triaxial shapes (i.e., including both  $\beta$  and  $\gamma$  deformations). The results reproduce available data and show that there is an abrupt change of structure at  $N = 90$  that can be approximately characterized by the  $X(5)$  analytic solution at the critical point of the first-order quantum phase transition between spherical and axially deformed shapes.

A phase transition is characterized by a significant variation of one or more order parameters as functions of the control parameter. Even though in systems composed of a finite number of particles (i.e., in mesoscopic systems) phase transitions are actually smoothed out, in many cases, clear signatures of abrupt changes of structure properties are observed. In their study of QPT transitions in mesoscopic systems [12], Iachello and Zamfir have shown that the main features of phase transitions, defined for an infinite number of particles,  $N \rightarrow \infty$ , persists even for moderate  $N \approx 10$ . Their analysis has been followed by several studies of shape phase-transitional patterns in nuclei as functions of the number of particles [e.g., number

of bosons in the framework of interacting-boson-type models (IBMs)]. As emphasized in Ref. [12], there are two approaches to study QPT: (i) the method of Landau, based on potentials, and (ii) the direct computation of order parameters. In the case of atomic nuclei, however, a quantitative analysis of QPT must go beyond a simple study of potential energy surfaces. This is because potentials or, more specifically, deformation parameters that characterize potential energy surfaces are not observables and can only be related to observables by making very specific model assumptions. The direct computation of observables related to order parameters has so far been based mostly on particular nuclear structure models (e.g., IBM), in the framework of which such observables are defined as expectation values of suitably chosen operators.

In this work, we combine both approaches in a consistent microscopic framework and present an illustrative example of calculation of observables that can be related to quantum order parameters as functions of the nucleon number. An order parameter is a measure of the degree of order in a system. As a normalized quantity that is zero in one (symmetric) phase, and nonzero in the other, it characterizes the onset of order at the phase transition. When symmetry is broken, several variables can be introduced, related to order parameters, to describe the state of the system. As in our previous studies [7,8], the shape transition in Nd isotopes with  $N \approx 90$  will be considered. The analysis starts by performing constrained self-consistent RMF calculations for triaxial shapes (i.e., including both  $\beta$  and  $\gamma$  deformations). The resulting self-consistent solutions (i.e., single-particle wave functions, occupation probabilities, and quasiparticle energies that correspond to each point on the binding energy surface) are used to calculate the parameters that determine the collective Hamiltonian: three mass parameters, three moments of inertia, and the zero-point energy corrections, as functions of the deformations  $\beta$  and  $\gamma$  [13]. The diagonalization of the Hamiltonian yields the excitation energies and collective wave functions that are used to calculate observables.

In Fig. 1, we plot the self-consistent triaxial quadrupole binding energy map of  $^{150}\text{Nd}$  in the  $\beta$ - $\gamma$  plane ( $0 \leq \gamma \leq 60^\circ$ ). The calculations are performed by imposing constraints

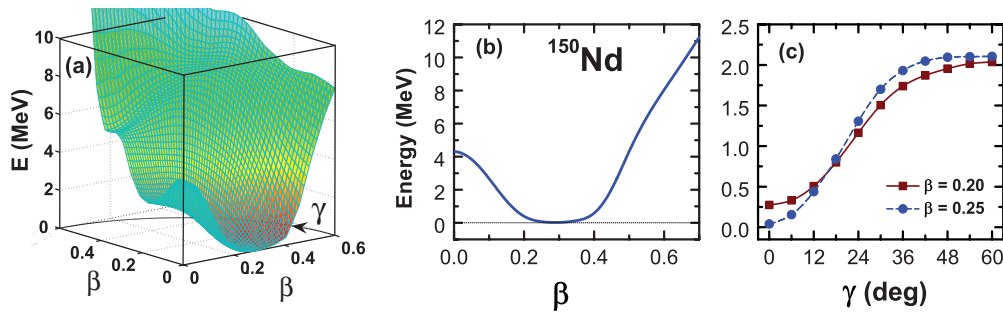


FIG. 1. (Color online) (a) Self-consistent RMF + BCS triaxial quadrupole binding energy map of  $^{150}\text{Nd}$  in the  $\beta$ - $\gamma$  plane ( $0 \leq \gamma \leq 60^\circ$ ). The contours join points on the surface with the same energy (in MeV). (b) Projection of the binding energy map on the  $\gamma = 0^\circ$  axis. (c) The dependence of the binding energy on the deformation parameter  $\gamma$ , for two values of the axial deformation  $\beta = 0.2$  and  $0.25$ .

on expectation values of the quadrupole moments  $\langle \hat{Q}_{20} \rangle$  and  $\langle \hat{Q}_{22} \rangle$ , the relativistic functional PC-F1 (point-coupling Lagrangian) [14] is used in the particle-hole channel, and a density-independent  $\delta$  force is the effective interaction in the particle-particle channel, with pairing correlations treated in the BCS approximation. As shown in Ref. [8], the binding energy maps of Nd isotopes show a gradual transition from lighter spherical nuclei toward the strongly prolate deformed  $^{152}\text{Nd}$ . Of particular interest are nuclei around  $^{150}\text{Nd}$ , for which experimental evidence for shape phase-transitional behavior has been reported [15].  $^{150}\text{Nd}$  is considered to be a good example of empirical realization of the X(5) model for the critical point of first-order phase transition between spherical and axially deformed shapes [16].

The microscopic binding energy surface of  $^{150}\text{Nd}$  displays a flat prolate minimum that extends in the interval  $0.2 \leq \beta \leq 0.4$  of the axial deformation parameter [Fig. 1(b)] and a parabolic dependence on  $\gamma$  for  $\gamma \leq 30^\circ$  in the region of the flat prolate minimum [Fig. 1(c)]. The flat bottom of the potential has been considered a signature of possible phase transition. There are, however, problems when one considers deformations as possible order parameters of phase transitions [10]. First, deformation parameters are not observables and can only be linked to observables (e.g., transition rates or excitation energies) within the framework of a specific model. Second, in calculations that include both  $\beta$  and  $\gamma$  degrees of freedom, a phase transition cannot be characterized by the behavior of just one deformation parameter (e.g.,  $\beta$ ). Results obtained with the five-dimensional collective Hamiltonian show that many properties of the excitation spectra are affected by  $\beta$ - $\gamma$  coupling. Bandhead excitation energies, energy spacings within the bands, and transition strengths depend on the  $\gamma$  stiffness of the potential [17].

Here we analyze observables that are directly computed using collective wave functions obtained from a microscopic five-dimensional collective Hamiltonian. The important question is how much are the discontinuities at a phase-transitional point smoothed out in finite nuclei, and second, how precisely can a point of phase transition be associated with a particular isotope, considering that the control parameter (i.e., nucleon number) is not continuous but takes only discrete integer values? Figure 2 displays the differences between squares of ground-state charge radii  $\langle r_c^2 \rangle_{0_1^+}(A+2) - \langle r_c^2 \rangle_{0_1^+}(A)$  and the

isomer shift  $\langle r_c^2 \rangle_{2_1^+} - \langle r_c^2 \rangle_{0_1^+}$  between the first  $2^+$  state and the ground state, as functions of the neutron number. The former displays a peak at  $N = 88$  and  $90$ , whereas a pronounced discontinuity is predicted for the latter between  $N = 88$  and  $N = 92$ .

Signatures of ground-state phase transitions in quantum systems characterize the evolution of both excitation spectra and order parameters. In Refs. [18–20], the scaling properties of the energy gap between the ground state and the first excited vibrational states with zero angular momentum were studied for a system of  $N_B$  interacting bosons. At the critical point of the phase transition, the gap is strongly reduced in finite systems and goes to zero as  $N \rightarrow \infty$ . In Fig. 3(a), we plot the isotopic dependence of the first and second excited  $0^+$  states in Nd nuclei and, in Fig. 3(b), the isomer shift  $\langle r_c^2 \rangle_{0_2^+} - \langle r_c^2 \rangle_{0_1^+}$ . The excitation energies of both  $0_2^+$  and  $0_3^+$  exhibit a pronounced dip at  $N = 90$ , which can be attributed to the softness of the potential with respect to  $\beta$  deformation in  $^{150}\text{Nd}$ . For lighter nuclei (i.e., toward spherical shapes),  $0_2^+$  and  $0_3^+$  display the structure of two- and three-phonon states, respectively. The axially deformed  $^{152,154,156}\text{Nd}$  are characterized by strong prolate minima and stiffer potentials, and the positions of  $\beta$  and  $\beta\beta$  bands are shifted to higher energies. This behavior

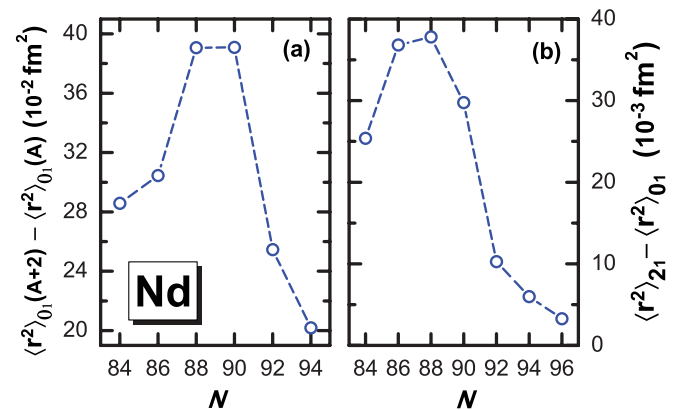


FIG. 2. (Color online) Calculated differences between squares of ground-state charge radii:  $\langle r_c^2 \rangle_{0_1^+}(A+2) - \langle r_c^2 \rangle_{0_1^+}(A)$  (a) and isomer shifts  $\langle r_c^2 \rangle_{2_1^+} - \langle r_c^2 \rangle_{0_1^+}$  (b) as functions of neutron number in Nd isotopes.

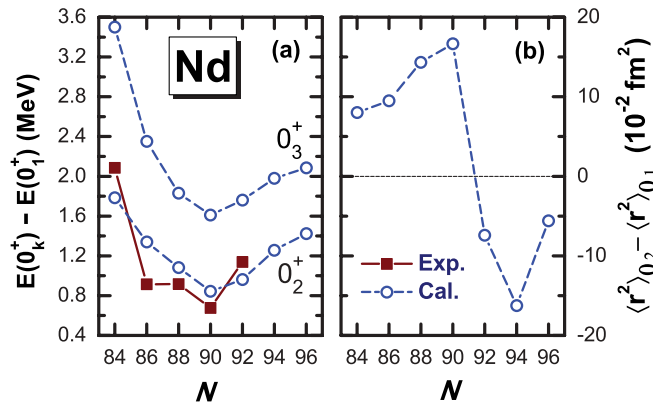


FIG. 3. (Color online) Evolution of the first and second excited  $0^+$  states (a) and the isomer shifts  $\langle r_c^2 \rangle_{0_2^+} - \langle r_c^2 \rangle_{0_1^+}$  (b) with the neutron number in Nd isotopes. Microscopic values calculated with the PC-F1 energy-density functional are compared with data [22].

of the  $0_2^+$  state in Nd-Sm-Gd isotopes was also predicted in the phenomenological analysis of the transition between the vibrational, SU(5), and the rotational, SU(3), limits of the IBM [21]. We note that, with the exception of the very low  $0_2^+$  state in  $^{146}\text{Nd}$ , the calculated excitation energies  $E_{0_2^+}$  are also in quantitative agreement with experimental values [22].

The microscopic calculation predicts a very interesting evolution of the isomer shift  $\langle r_c^2 \rangle_{0_2^+} - \langle r_c^2 \rangle_{0_1^+}$ . After a steep rise in neutron number for  $N \leq 90$ , the isomer shift actually changes sign between  $N = 90$  and  $N = 92$  (i.e., in  $^{152,154,156}\text{Nd}$ , the charge radius of the  $0_2^+$  state is smaller than that of the ground state). As a function of the control parameter (number of neutrons), the isomer shift displays a behavior characteristic for a first-order phase transition [12]. Evidence for deformation crossing near the first-order shape phase transition in  $^{152-156}\text{Gd}$  has recently been reported in a study that used experimental  $B(E2)$  values to extract the model-independent quadrupole shape invariants, which provide a measure of the  $\beta$  deformation [23]. Note that, although the results correspond to a realistic calculation of ground-states and collective excitation spectra of Nd nuclei, both isomer shifts (i.e.,  $\langle r_c^2 \rangle_{2_1^+} - \langle r_c^2 \rangle_{0_1^+}$  and  $\langle r_c^2 \rangle_{0_2^+} - \langle r_c^2 \rangle_{0_1^+}$ ) exhibit very sharp discontinuities at  $N = 90$ . The first-order phase transition appears not to be smoothed out by the finiteness of the nuclear system. In general, the characteristic behavior of order parameters at the point of QPT is more pronounced than in the case of Ising-type Hamiltonians representing systems of interacting bosons, especially for a realistic number of bosons (i.e.,  $N_B \approx 5-10$  for medium-heavy nuclei). In the latter case, the discontinuities are smoothed out so that, qualitatively, a first-order phase transition might actually appear like a second-order one [12].

Shape transitions and change in radii are also reflected in the transition matrix elements of the electric monopole  $\hat{T}(E0)$  operator [24]. In the study of sharply rising  $E0$  strength in transitional nuclei [25], based on a general IBM Hamiltonian of Ising-type, it has been shown that  $0_2^+ \rightarrow 0_1^+$  transitions provide a clear signature of phase-transitional behavior in finite nuclei. In shape transition regions,  $\rho^2(E0; 0_2^+ \rightarrow 0_1^+)$  displays a steep rise and then remains large for well-deformed

nuclei. Relative and absolute  $E0$  transition strengths on the transitional path between the  $X(5)$  solution and the rigid rotor limit have recently been evaluated using the confined  $\beta$ -soft (axially symmetric) rotor model [26], and it has been shown that absolute  $E0$ -transition strengths are reduced with increasing potential stiffness toward zero in the rigid-rotor limit.

The  $E0$  operator can be expressed in terms of single-nucleon degrees of freedom as  $\hat{T}(E0) = \sum_k e_k r_k^2$ , where  $e_k$  is the charge of the  $k$ th nucleon and  $r_k$  is its position relative to the center of mass of the nucleus. For the transition  $0_2^+ \rightarrow 0_1^+$ , the absolute  $E0$  strength is defined as

$$\rho^2(E0; 0_2^+ \rightarrow 0_1^+) = \left| \frac{\langle 0_2^+ | \hat{T}(E0) | 0_1^+ \rangle}{eR^2} \right|^2, \quad (1)$$

where  $R$  is the nuclear radius,  $R \simeq 1.2A^{1/3}$  fm. Figure 4 shows the calculated values  $\rho^2(E0; 0_2^+ \rightarrow 0_1^+)$  as a function of neutron number  $N$ . Bare charges have been used in the calculation (i.e.,  $e_p = e$  and  $e_n = 0$ ). The monopole transition strengths exhibit a markedly sharp increase toward the point of phase transition at  $N = 90$ , and the  $\rho^2(E0; 0_2^+ \rightarrow 0_1^+)$  values remain rather large in the well-deformed nuclei  $^{152,154,156}\text{Nd}$ , which is a result similar to that obtained in the schematic IBM calculation of Ref. [25]. This behavior of  $\rho^2(E0; 0_2^+ \rightarrow 0_1^+)$  is characteristic for an order parameter at the point of first-order QPT. In terms of absolute values, one notes that even without introducing effective charges, the calculated  $\rho^2(E0; 0_2^+ \rightarrow 0_1^+)$  are in qualitative agreement with the available experimental values for Sm and Gd nuclei [24].

In conclusion, a microscopic calculation of observables related to order parameters for a first-order nuclear QPT between spherical and axially deformed shapes has been performed. Starting from self-consistent triaxial mean-field binding energy maps in the  $\beta$ - $\gamma$  plane for a sequence of even-even Nd isotopes with neutron number  $N = 84-96$ , a set of observables has been computed using collective wave functions obtained by diagonalization of the corresponding five-dimensional

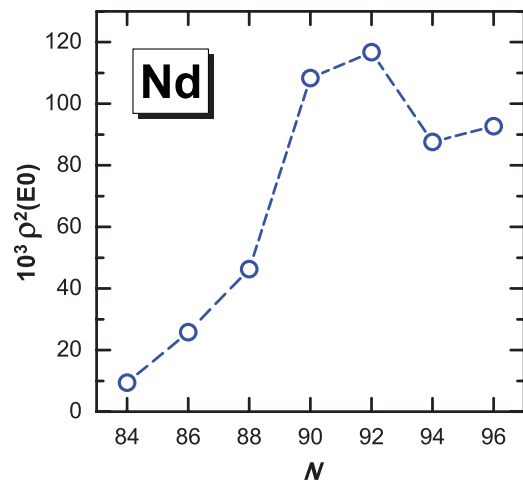


FIG. 4. (Color online) The calculated monopole transition strength  $\rho^2(E0; 0_2^+ \rightarrow 0_1^+)$  as a function of neutron number  $N$  in Nd isotopes.

Hamiltonian for quadrupole vibrational and rotational degrees of freedom. The energy gap between the ground state and the excited vibrational states with zero angular momentum, the isomer shifts  $\langle r_c^2 \rangle_{2_1^+} - \langle r_c^2 \rangle_{0_1^+}$  and  $\langle r_c^2 \rangle_{0_2^+} - \langle r_c^2 \rangle_{0_1^+}$ , and the monopole transition strengths  $\rho^2(E0; 0_2^+ \rightarrow 0_1^+)$  exhibit pronounced discontinuities at  $N = 90$ , which are characteristic of first-order QPTs. Even though the calculation has been carried out for a finite number of nucleons, the phase transition does not appear to be significantly smoothed out by the finiteness of the nuclear system. Together with the results reported in Refs. [7] and [8], our analysis has shown that the microscopic framework based on universal energy-density functionals

provides a fully consistent description of nuclear-shape QPT in the rare-earth region around  $N = 90$ .

We thank R. F. Casten, F. Iachello, and N. Pietralla for useful discussions. This work was supported in part by MZOS Project No. 1191005-1010, by the Major State 973 Program 2007CB815000, and the NSFC under Grant No. 10775004. The work of J.M., T.N., and D.V. was supported in part by the Chinese-Croatian project “Nuclear structure far from stability.” T. N. acknowledges support from the Croatian National Foundation for Science, Higher Education and Technological Development.

- 
- [1] F. Iachello, in *Proceedings of the International School of Physics “Enrico Fermi” Course CLIII*, edited by A. Molinari, L. Riccati, W. M. Alberico, and M. Morando (IOS Press, Amsterdam, 2003).
- [2] R. F. Casten and E. A. McCutchan, *J. Phys. G: Nucl. Part. Phys.* **34**, R285 (2007).
- [3] P. Cejnar and J. Jolie, *Prog. Part. Nucl. Phys.* **62**, 210 (2009).
- [4] J. Meng, W. Zhang, S. G. Zhou, H. Toki, and L. S. Geng, *Eur. Phys. J. A* **25**, 23 (2005).
- [5] Z.-Q. Sheng and J.-Y. Guo, *Mod. Phys. Lett. A* **20**, 2711 (2005).
- [6] R. Fossion, D. Bonatsos, and G. A. Lalazissis, *Phys. Rev. C* **73**, 044310 (2006).
- [7] T. Nikšić, D. Vretenar, G. A. Lalazissis, and P. Ring, *Phys. Rev. Lett.* **99**, 092502 (2007).
- [8] Z. P. Li, T. Nikšić, D. Vretenar, J. Meng, G. A. Lalazissis, and P. Ring, *Phys. Rev. C* **79**, 054301 (2009).
- [9] R. Rodríguez-Guzmán and P. Sarriguren, *Phys. Rev. C* **76**, 064303 (2007).
- [10] T. R. Rodríguez and J. L. Egido, *Phys. Lett.* **B663**, 49 (2008).
- [11] L. M. Robledo, R. Rodríguez-Guzmán, and P. Sarriguren, *Phys. Rev. C* **78**, 034314 (2008).
- [12] F. Iachello and N. V. Zamfir, *Phys. Rev. Lett.* **92**, 212501 (2004).
- [13] T. Nikšić, Z. P. Li, D. Vretenar, L. Próchniak, J. Meng, and P. Ring, *Phys. Rev. C* **79**, 034303 (2009).
- [14] T. Bürvenich, D. G. Madland, J. A. Maruhn, and P.-G. Reinhard, *Phys. Rev. C* **65**, 044308 (2002).
- [15] R. Krücken *et al.*, *Phys. Rev. Lett.* **88**, 232501 (2002).
- [16] F. Iachello, *Phys. Rev. Lett.* **87**, 052502 (2001).
- [17] M. A. Caprio, *Phys. Rev. C* **72**, 054323 (2005).
- [18] D. J. Rowe, P. S. Turner, and G. Rosensteel, *Phys. Rev. Lett.* **93**, 232502 (2004).
- [19] S. Dusuel, J. Vidal, J. M. Arias, J. Dukelsky, and J. E. García-Ramos, *Phys. Rev. C* **72**, 011301(R) (2005).
- [20] J. M. Arias, J. Dukelsky, J. E. García-Ramos, and J. Vidal, *Phys. Rev. C* **75**, 014301 (2007).
- [21] O. Scholten, F. Iachello, and A. Arima, *Ann. Phys. (NY)* **115**, 325 (1978).
- [22] NNDC National Nuclear Data Center, Brookhaven National Laboratory (<http://www.nndc.bnl.gov/>).
- [23] V. Werner, E. Williams, R. J. Casperson, R. F. Casten, C. Scholl, and P. von Brentano, *Phys. Rev. C* **78**, 051303(R) (2008).
- [24] J. L. Wood, E. F. Zganjar, C. De Coster, and K. Heyde, *Nucl. Phys.* **A651**, 323 (1999).
- [25] P. von Brentano, V. Werner, R. F. Casten, C. Scholl, E. A. McCutchan, R. Krücken, and J. Jolie, *Phys. Rev. Lett.* **93**, 152502 (2004).
- [26] J. Bonnet, A. Krugmann, J. Beller, N. Pietralla, and R. V. Jolos, *Phys. Rev. C* **79**, 034307 (2009).